We are IntechOpen, the world's leading publisher of Open Access books Built by scientists, for scientists

4,800
Open access books available

122,000
International authors and editors

135M
Downloads

Our authors are among the

154
Countries delivered to

TOP 1%
most cited scientists

12.2%
Contributors from top 500 universities

CLARIVATE ANALYTICS BOOK CITATION INDEX INDEXED

WEB OF SCIENCE™

Selection of our books indexed in the Book Citation Index in Web of Science™ Core Collection (BKCI)

Interested in publishing with us?
Contact book.department@intechopen.com

Numbers displayed above are based on latest data collected.
For more information visit www.intechopen.com

Chapter 4

Assessment of Reservoir Sedimentation Effect on Coastal Erosion and Evaluation of Sediment Removal Techniques for Its Reduction — The Case of Nestos River, Greece

Manolia Andredaki, Anastasios Georgoulas, Vlassios Hrissanthou and Nikolaos Kotsovinos

Additional information is available at the end of the chapter

http://dx.doi.org/10.5772/61459

Abstract

Nestos is one of the most important transboundary rivers flowing through Bulgaria and Greece. In the Greek part of the river, two reservoirs, the Thisavros Reservoir and the Platanovrysi Reservoir, have already been constructed and started operating in 1997 and 1999, respectively. In the first part of the chapter, the reservoir sedimentation effect on the coastal erosion is investigated, for the case of the Nestos River delta and the adjacent shorelines, through a combination of mathematical modeling, modern remote sensing techniques, and field surveying, while in the second part, the mechanical removal as well as the flushing of sediment from the reservoir of Platanovrysi and its disposal in the subbasin downstream of the Platanovrysi Dam up to the Nestos River delta are investigated as potential treatment methods of reducing coastal erosion, using a modification of the same mathematical model that is utilized in the first part of the chapter. The overall findings and conclusions arising from the work presented and discussed in the present chapter contribute to the overall need to thoroughly understand the direct effect of dam construction on coastal erosion, as well as to examine the effectiveness of potential sediment management treatments.

Keywords: Sediment transport/management, reservoir, mathematical modeling, coastal erosion, shoreline change monitoring, Nestos River

1. Introduction

Coastal erosion constitutes a major environmental problem in many parts of the world. Especially in deltaic regions, the construction of dams in the river basin acts as an artificial barrier to the sediment supply to the river mouths and therefore the rates of shoreline retreat and sea level rise may exceed the corresponding rates of vertical shoreline accretion, resulting in the increase and in many cases the predomination of deltaic and coastal erosion. Over the last decades, many investigations have been directly or indirectly focused on the assessment of reservoir sedimentation and its effect on sediment yield reduction and coastal erosion, in the wider coastal regions of various rivers worldwide, using different investigation methodologies and techniques (e.g., [1]-[8]).

Nestos constitutes an important transboundary river, characterized by its great biodiversity. It flows through two European countries, Bulgaria and Greece, discharging into the Aegean Sea. It originates from Mount Rila (2716 m) in South Bulgaria, where Nestos River is known as Mesta. Its total length reaches 234 km and the river basin covers an area of 5749 km^2, 130 km (<56%) and 2280 km^2 (<40%) of which lies in Greek territory [9].

In the Greek part of the river, two hydroelectric dams, the Thisavros Dam and the Platanovrysi Dam, have already been constructed and started operating in 1997 and 1999, respectively. This implies a reduction of sediment yield at the outlet of the Nestos River basin and a corresponding disturbance of the sediment balance in the basin in general, which can result in coastal erosion. However, the reduction of the sediment yield at the outlet of the considered river due to the construction of these two reservoirs as well as the increase in the coastal erosion of the deltaic and the adjacent coastal regions have never been evaluated and correlated previously.

According to the authors' best knowledge, the work that is presented in the first part of this chapter constitutes one of the first assessments of reservoir sedimentation effect on the coastal erosion for the case of the Nestos River delta and the adjacent shorelines, utilizing mathematical modeling, remote sensing techniques, and field surveying [10]. The main objectives are to evaluate the overall reduction of the sediment yield at the outlet of the river due to the construction of the two dams and to examine the resulting erosion/accretion response of the deltaic as well as the adjacent shorelines. For this purpose, the sediment yield at the outlet of the Nestos River basin before and after the construction of the two dams is calculated, through the application of a mathematical simulation model (RUNERSET – RUNoff ERosion SEdiment Transport). The model is initially tested against appropriate field measurements that are available in the literature. Moreover, a shoreline change monitoring methodology for the coastal region of the Nestos River delta and the adjacent shorelines is proposed, tested, and applied for the digital and detailed extraction of the shoreline position with respect to time, aiming to determine the erosion/accretion shoreline balance for two time periods that correspond to the periods before and after the construction of the dams. Finally, the mathematically calculated reduction of the sediment yield at the outlet of the river is correlated with the results from the application of the shoreline change monitoring methodology and some valuable conclusions and recommendations are drawn. The considered mathematical simulation model (RUNERSET) calculates the mean annual value of sediment yield, due to rainfall and runoff.

http://dx.doi.org/10.5772/61459

The proposed model consists of three submodels: a rainfall-runoff submodel, a soil erosion submodel and a sediment transport submodel for streams. The coastal erosion/accretion monitoring data that were used in order to determine the shoreline evolution consist of remote sensing data from high-resolution satellite images (year 2002, considered period of construction/operation of the dams) and aerial photographs (year 1945, period before the construction/operation of the dams/reservoirs) as well as from high-resolution DGPS (Differential Global Positioning System) field measurements (year 2007, period after the construction/operation of the dams/reservoirs). It is calculated that the construction and operation of the considered dams have caused a dramatic decrease (about 83%) in the sediments supplied directly to the basin outlet and indirectly to the neighboring coast, and that this fact has almost inversed the erosion/accretion balance in the deltaic as well as the adjacent shorelines. Before the construction of the reservoirs, in the entire pilot study region, accretion predominated erosion by 25.36%, while just within 5 years of the construction/operation of the reservoirs, erosion predominates accretion by 21.26% [10]. Moreover, in the same part of this chapter, aiming to quantitatively investigate the dynamic evolution of erosion in the considered coastal region, a more recent shoreline (2013) was also extracted. For this purpose, additional DGPS field measurements were performed, following the same methodology and time period (spring) with the corresponding field measurements of the year 2007. Recording this more recent state of the coastline (2013) and comparing with the previous shorelines up to the perceived period of the construction and operation of the dams (2002) showed that erosion, in relation to the deposition/accretion that has been observed in the period 2002-2007, shows an increasing trend.

It has been estimated that every year almost 2% of the effective volume of reservoirs worldwide is lost due to sedimentation. This is an unavoidable fact, which however can be reduced, quantified, and incorporated into the design and operation of a reservoir [11]. The sediment management methods in reservoirs can be classified into three main categories: a) methods that minimize the inflow of sediment into the reservoirs, b) methods that minimize the accumulation of sediment in the upstream part of the reservoir and c) methods that maximize the overall sediment discharge that passes downstream of the reservoirs. The application of this last class of methods could serve as a possible treatment for the reduction of shoreline erosion, which has been mainly caused by the construction of the above-mentioned dams in the case of Nestos River. Two of the most widely applied methods of sediment removal from reservoirs are the processes of mechanical removal or dredging [11] and flushing [12]. In the work that is presented in the second part of this chapter, the dredging as well as the flushing of sediment from the reservoir of Platanovrysi, and its disposal in the subbasin downstream of the Platanovrysi Dam up to the Nestos River delta, are investigated as potential treatment methods of reducing coastal erosion ([13], [14]). For this purpose, the considered mathematical model (RUNERSET) was accordingly modified in order to incorporate these effects, and various scenarios of sediment management in the Platanovrysi Reservoir were simulated, while an assessment of the most effective and consistent month of the year for sediment flushing or dredging, as well as of the maximum transport quantity of the removed material was conducted. Finally, a comparison of the two methods takes place, concerning the maximum sediment quantities that reach the basin outlet, at the optimal for each method month of the year.

The overall findings and conclusions, arising from the work presented and discussed in this chapter, contribute to the need to thoroughly understand the direct effect of dam construction on coastal erosion. More specifically, the presented work constitutes one of the first attempts to quantify the disruption of the sediment balance in the delta of Nestos River due to the construction and operation of the Thisavros and Platanovrysi Reservoirs, considering simultaneously the impact of this disturbance on the erosion/accretion balance both at the river delta and the adjacent shorelines. Moreover, for the first time, an effort is made for the evaluation of the optimum periods and sediment management methods, aiming to increase the annual sediment that reaches the outlet of the Nestos River basin, and consequently to reduce erosion in the delta of the river and the adjacent shorelines. Finally, it is evident that the overall research methodology applied may constitute a quite useful tool for the further investigation of the effect of dam construction on the coastal erosion for other pilot application areas, throughout the world.

2. Assessment of reservoir sedimentation effect on coastal erosion

2.1. Description of the mathematical simulation model

As mentioned previously in the introduction section of this chapter, the considered mathematical simulation model (RUNERSET) calculates the mean annual value of sediment yield, due to rainfall and runoff, and it consists of three submodels: a rainfall-runoff submodel, a soil erosion submodel, and a sediment transport submodel for streams.

By means of the rainfall-runoff submodel, the runoff depth for a certain rainfall depth is computed. It is a simplified water balance model [15], in which the variation of soil moisture due to rainfall, evapotranspiration, deep percolation, and runoff is considered. The basic balancing equation is:

$$S_n' = S_{n-1} + N_n - E_{pn} \tag{1}$$

where S_{n-1} is the available soil moisture for the time step $n-1$ (mm); $N_n$is the rainfall depth for the time step n (mm); $E_{pn}$is the potential evapotranspiration for the time step n (mm); and S_n' is an auxiliary variable (mm).

The direct runoff depth h_{on} (mm) and the deep percolation IN_n (mm) for the time step n can be evaluated by comparing S_n' with the maximum available soil moisture S_{max} (mm), which is estimated by the following relationship of the US Soil Conservation Service [16]:

$$S_{\max} = 25.4[(1000/CN) - 10] \tag{2}$$

where CN is the curve number depending on the soil cover, the hydrologic soil group, and the antecedent soil moisture conditions ($0 < CN < 100$).

http://dx.doi.org/10.5772/61459

In the present study, two different methods were used for the estimation of the potential evapotranspiration E_p : the radiation method improved by Doorenbos and Pruitt [17] was used for the Greek part of the Nestos River basin, while the Thornthwaite method [18] was used for the Bulgarian part of the Nestos River basin.

The following meteorological data are required for the application of the radiation method: mean daily temperature (°C), sunlight hours per day (hr/day), mean daily relative humidity (%), and mean daily wind velocity (m/s). These data were available in the Greek part of Nestos River basin. For the application of the Thornthwaite method, only mean daily temperature data (°C) are required, which were available in the Bulgarian part of the Nestos River basin.

According to the equations given above, apart from the meteorological data, the input data for the rainfall-runoff submodel are: monthly rainfall depth, altitude, latitude, soil cover – land use, and hydrologic soil group.

The soil erosion submodel is based on the assumption that the impact of droplets on the soil surface and the surface runoff are proportional to the momentum flux contained in the droplets and the runoff, respectively [19].

The momentum flux exerted by the falling droplets, ϕ_r(kg m/s^2), is given by:

$$\phi_r = Cr\rho A u_r \sin a \tag{3}$$

where C is the soil cover factor; $r$is the rainfall intensity (m/s); $\rho$is the water density (kg/m^3); $A$is the subbasin area (m^2); u_r is the mean fall velocity of the droplets (m/s); and α is the mean slope angle of the soil surface (°).

The original relationship of Schmidt for the momentum flux exerted by the droplets is valid for bare soils. Therefore, an additional factor is necessary to express the decrease of the momentum flux because of the vegetation. It is believed that the dimensionless crop and management factor C of the USLE (Universal Soil Loss Equation) is appropriate to express the vegetation influence.

The momentum flux exerted by the runoff, ϕ_f (kg m/s^2), is given by:

$$\phi_f = q\rho b u \tag{4}$$

where q is the direct runoff rate per unit width [m^3/(s m)]; $b$is the width of the subbasin area (m); and u is the mean flow velocity (m/s).

The available sediment discharge per unit width, q_{rf} [(kg/(m s)], due to rainfall and runoff, in the subbasin considered is given by [19]:

$$q_{rf} = (1.7E - 1.7)10^{-4} \tag{5}$$

where

$$E = (\phi_r + \phi_f) / \phi_{cr} \quad (E > 1) \tag{6}$$

and ϕ_{cr} is the critical momentum flux (kg m/s^2).

The critical momentum flux ϕ_{cr}, which designates the soil erodibility, can be calculated from:

$$\phi_{cr} = q_{cr} \rho b u \tag{7}$$

where q_{cr} [m^3/(s m)] is the direct runoff rate per unit width at initial erosion.

The critical runoff rate q_{cr} is determined from the critical erosion velocity depending on soil roughness.

Equation (6) suggests the concept of critical situation characterizing the initiation of sediment motion on the soil surface.

The sediment supply ES [(kg/(s m)] to the main stream of the subbasin considered is estimated by means of a comparison between the available sediment discharge q_{rf} in the subbasin and the sediment transport capacity by overland flow per unit width, q_t[kg/(s m)], which is computed as follows [19]:

$$q_t = c_{\max} \rho_s q \tag{8}$$

where c_{max} is the concentration of suspended particles at transport capacity (m^3/m^3); $\rho_s$is the sediment density (kg/m^3).

The additional input data for the soil erosion submodel, with reference to the rainfall-runoff submodel, are: mean slope angle of soil surface, subbasin area, soil cover factor, length of the main stream of the subbasins, roughness coefficient of soil surface, critical erosion velocity, water, and sediment density.

The sediment yield at the outlet of the main stream of the subbasin considered can be computed by the concept of sediment transport capacity by the stream flow. The following relationships are used to compute sediment transport capacity by the stream flow [20]:

$$\begin{aligned} \log c_t &= 5.435 - 0.286 \log \frac{wD_{50}}{\nu} - 0.457 \log \frac{u_*}{w} + \\ &+ (1.799 - 0.409 \log \frac{wD_{50}}{\nu} - 0.314 \log \frac{u_*}{w}) \log (\frac{us}{w} - \frac{u_{cr} s}{w}) \end{aligned} \tag{9}$$

http://dx.doi.org/10.5772/61459

$$\frac{u_{cr}}{w} = \frac{2.5}{\log(u_* D_{50} / \nu) - 0.66}, \text{ if } 1.2 < u_* D_{50} / \nu < 70 \tag{10}$$

$$\frac{u_{cr}}{w} = 2.05, \text{ if } \frac{u_* D_{50}}{\nu} \geq 70 \tag{11}$$

where c_t is the total sediment concentration by weight (ppm); $w$is the terminal fall velocity of suspended particles (m/s); $D_{50}$is the median grain diameter of the bed material (m); $\nu$is the kinematic viscosity of the water (m^2/s); $u_*$is the shear velocity (m/s); $u$is the mean flow velocity (m/s); $u_{cr}$is the critical mean flow velocity (m/s); and s is the energy slope.

Equation (9) was determined from the concept of unit stream power (rate of potential energy expenditure per unit weight of water,us) and dimensional analysis. The variable u_{cr} in Equation (9) suggests that a critical situation is considered at the beginning of sediment particle motion, as in most sediment transport equations.

The sediment yield *FLO* [kg/(s m)] at the outlet of the main stream of the subbasin considered can be estimated by comparing the available sediment in the stream, *ESI* [kg/(s m)], with the transport capacity by the stream flow, q_{ts}[kg/(s m)], resulting from the total sediment concentrationc_t.

It is implied from the above relationships that only the main stream of each subbasin is considered, because numerous unavailable data for the geometry and hydraulics of the entire stream system would otherwise be required. Therefore, the additional input data for the stream sediment transport submodel, with reference to the foregoing submodels, concern the main stream of the subbasins: base flow, bottom slope, bottom width, bed roughness, diameter of suspended particles, grain diameter of bed material, and kinematic viscosity of water.

Finally, a sediment routing plan is necessary in order to specify the sediment motion from subbasin to subbasin.

2.2. Application of the simulation model

2.2.1. Available data and maps for Nestos River basin

For more precise calculations, the Nestos River basin was divided into 60 subbasins. In more detail, the basin of the Thisavros Reservoir (Bulgarian and Greek parts) was divided into 31 subbasins, the basin of the Platanovrysi Reservoir (Greece) into nine subbasins and the basin downstream of the Platanovrysi Reservoir into 20 subbasins. The outlet of the last basin is known as Toxotes outlet.

Available meteorological data (monthly rainfall data and mean monthly temperature data) from 22 meteorological stations in Greece and Bulgaria were used as input data for the

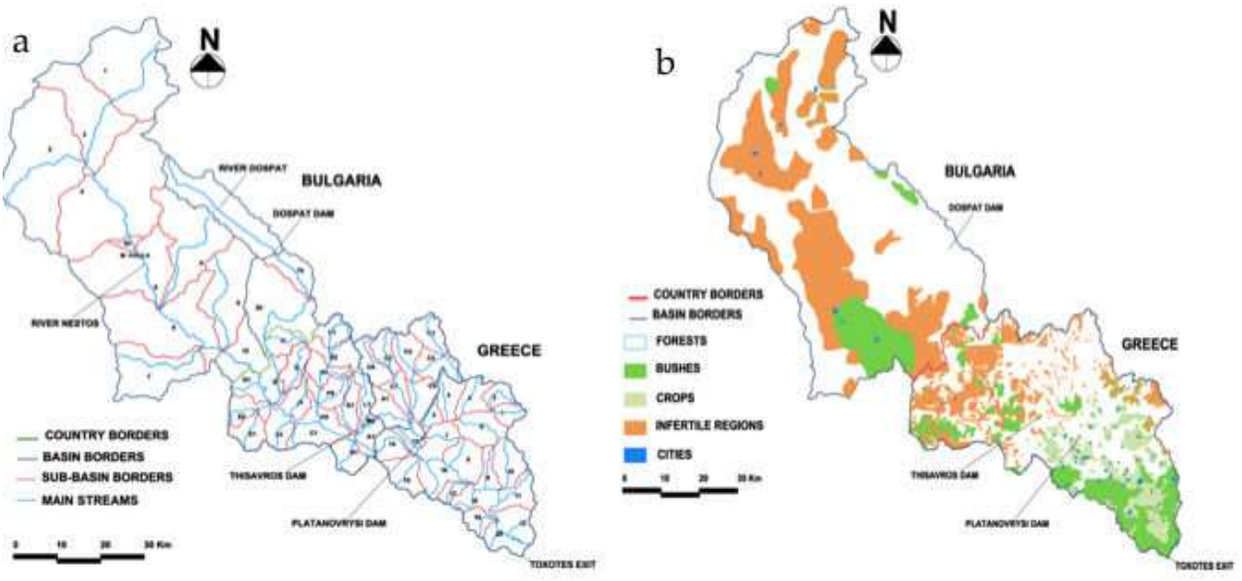

Figure 1. Subbasins/main streams map and soil cover map of the Nestos River basin

simulation model. Various digital thematic maps were constructed from georeferenced background maps, for the accurate computation of the required input parameters. Indicatively, the subbasins and main streams map as well as the soil cover map are depicted in Figure 1.

However, other kind of thematic maps were also constructed and used such as a Thiessen polygons map and a geological map. The calculations were performed on a monthly time basis for each subbasin.

2.2.2. Model testing

In order to validate the mathematical model predictions, sediment measurements (suspended load) for 53 years (1937-1989) that were available for the location "Momina Koula" [21] in the Bulgarian part of Nestos River (Figure 1), were utilized. According to the measurements, the mean annual suspended sediment yield for the considered time period is 202 t/km^2 [21]. Bed load measurements were not available and therefore, the following assumption [10] was made: the ratio of bed load to suspended load at the outlet of a basin on an annual basis amounts approximately to 0.25. According to this assumption, the measured mean annual sediment yield at "Momina Koula" is 252.5 t/km^2.

The mathematical model described in the previous section was applied to the basin corresponding to this location for the same time period [10]. The basin area is 1511 km^2, which is about 30% of the entire basin area of the Nestos River. The results of the model application for the different years are given in Table 1.

The mean annual value of sediment yield at the basin outlet, according to Table 1, is 315 000 t or 207.9 t/km^2. This means that the mathematical model underestimates the measured mean annual sediment yield by about 18%. However, taking into account the overall assumptions

http://dx.doi.org/10.5772/61459

Year	Annual sediment yield (t)	Year	Annual sediment yield (t)	Year	Annual sediment yield (t)	Year	Annual sediment yield (t)
1937	366 000	1950	278 500	1964	91 000	1977	85 500
1938	300 500	1951	428 500	1965	276 500	1978	280 500
1939	271 500	1952	374 000	1966	475 500	1979	315 000
1940	447 500	1953	359 000	1967	107 500	1980	314 000
1941	144 500	1954	786 000	1968	252 500	1981	200 500
1942	313 500	1955	381 000	1969	634 500	1982	209 500
1943	36 000	1956	458 000	1970	152 500	1983	68 500
1944	327 000	1958	413 000	1971	511 500	1984	185 000
1945	485 000	1959	274 000	1972	179 000	1985	239 000
1946	338 000	1960	555 500	1973	318 000	1986	511 000
1947	517 500	1961	160 500	1974	225 000	1987	288 500
1948	72 000	1962	798 500	1975	55 500	1988	253 000
1949	230 500	1963	705 500	1976	319 500	1989	7 500

Table 1. Computational results of sediment yield for the location "Momina Koula"

of the mathematical model as well as the complexity of the simulated process, these arithmetic predictions can be considered to be acceptable.

The relatively low deviation between computation and measurement results for the mean annual sediment yield at the location "Momina Koula" was an encouraging indication for the further application of the simulation model to other parts of the Nestos River basin. The following calculations were therefore performed for a time period of 11 years (1980-1990), which corresponds to the period before the construction and operation of the considered reservoirs:

- Calculation of mean annual sediment amount inflowing into the Thisavros Reservoir from the Bulgarian part (3052 km^2) and from the Greek part (804 km^2) of the Nestos River basin ([10]; [22])
- Calculation of mean annual sediment amount inflowing into the Platanovrysi Reservoir from the corresponding basin (405 km^2, Greece) [23]

In a previous study [24], the mean annual value of sediment yield at the outlet of the Nestos River basin (Toxotes) was calculated. Due to the construction and operation of the considered reservoirs, the sediment yield originates mainly from the part of the Nestos River basin which lies downstream of the Platanovrysi Reservoir (840 km^2, Greece).

The calculated values of the annual sediment yield for different years at certain locations of the Nestos River basin (Thisavros Reservoir, Platanovrysi Reservoir, and Toxotes) are summarized in Table 2.

Year	Basin of Thisavros Reservoir (Bulgarian part) (t)	Basin of Thisavros Reservoir (Greek part) (t)	Basin downstream of Dospat Reservoir (t)	Basin of Platanovrysi Reservoir (t)	Basin downstream of Platanovrysi Reservoir (t)	Entire basin of Nestos River (t)
1980	1 084 000	184 000	154 500	366 000	278 000	2 066 500
1981	968 000	128 000	128 500	344 000	588 000	2 156 500
1982	850 000	312 500	112 500	409 000	426 000	2 110 000
1983	309 500	114 000	32 500	99 500	73 000	628 500
1984	678 500	360 500	107 500	277 000	494 000	1 917 500
1985	991 000	94 500	127 500	54 500	131 000	1 398 500
1986	1 495 500	613 000	162 000	303 500	198 000	2 772 500
1987	1 021 000	875 500	131 500	761 500	673 000	3 462 500
1988	884 000	357 500	130 000	241 000	383 000	1 995 500
1989	73 500	121 000	xx	192 500	207 000	594 000
1990	545 500	552 500	46 500	289 500	64 000	1 498 000
Mean value	809 000	337 500	113 000	314 500	331 000	1 873 000

Table 2. Computational results of sediment yield at various locations of the Nestos River basin

2.2.3. Main computations of sediment yield for the Nestos River Basin

For these calculations, the major assumption is that all sediments inflowing into the reservoirs are deposited in the reservoirs, which represents the most unfavorable case regarding coastal erosion. According to Table 2, the mean annual value of sediment yield at the outlet of the Nestos River basin before the construction of the dams (mean annual value of sediment yield at the outlet of the entire Nestos River basin) is about 1.9×10^6 t, while after the construction of the dams (mean annual value of sediment yield at the outlet of basin downstream of the Platanovrysi Reservoir) this amounts to 0.33×10^6 t. Therefore, it is evident that the construction and operation of the considered reservoirs has caused a dramatic decrease, of about 83%, in the sediments supplied directly to the basin outlet and indirectly to the neighboring coast. Since Nestos River constitutes one of the main sediment supply sources for the west and east parts of the coastal region in the vicinity of its delta, it is expected that the calculated reduction in the sediment yield that reaches the Nestos River mouth will influence the seashore sediment balance, and it may result in a considerable increase in the erosion rates of the Nestos River mouth and the adjacent shorelines.

http://dx.doi.org/10.5772/61459

2.3. Description and testing of adopted methodology for shoreline change monitoring

2.3.1. Overview

The adopted shoreline change monitoring methodology for the Nestos River delta and the adjacent shorelines was the use of available high-resolution satellite images from the QuickBird (QB) satellite archive and aerial photographs from the Hellenic Military Geographical Service (HMGS), in conjunction with high-resolution GPS field measurements of the region [10]. In more detail:

- Use of ortho-rectified/georeferenced satellite images that were available in the QB archive for the extraction of the shoreline in the year 2002. The spatial resolution of these satellite images is 0.6 m per pixel. The proposed year was selected, as it was more close to the years 1997 and 1999 of the construction and operation of the considered reservoirs.
- Use of high-resolution DGPS field measurements for the extraction of the shoreline in the year 2007, in order to obtain the shoreline state approximately a decade after the operation of the considered reservoirs. The accuracy of these field measurements can reach the order of few centimeters.
- Comparison of the extracted shorelines between these 2 years in order to access a short-term shoreline evolution of the region that can be considered to be the period after the construction of the dams.
- Ortho-rectification/georeferencing of available, old aerial photographs of the region from the year 1945 from the HMGS and extraction of an old shoreline, approximately 50 years before the construction and operation of the reservoirs.
- Comparison of the extracted shorelines between the years 1945 and 2002 in order to access a long-term shoreline evolution of the region that can be considered to be the period before the construction of the dams.

In order to test the accuracy of the adopted shoreline change monitoring methodology, this was first applied to a small part of the total pilot study region (Figure 2). The proposed test part is composed by the mainland shoreline at the west of Nestos River delta extending from the Akroneri Cape until the Keramoti Bay.

The main steps of the utilized methodology are outlined in the following subsections.

2.3.2. Creation of common working background

In order to use a common working subbase, an ortho-rectified background of the wider geographical region was created using various available topographic maps from the HMGS. The merging and ortho-rectification of the proposed maps was conducted in ArcMap software from the ArcGIS 9 package, using as Ground Control Points (GCPs) a wide number of known, benchmark trigonometric points of the region that were available by the HMGS.

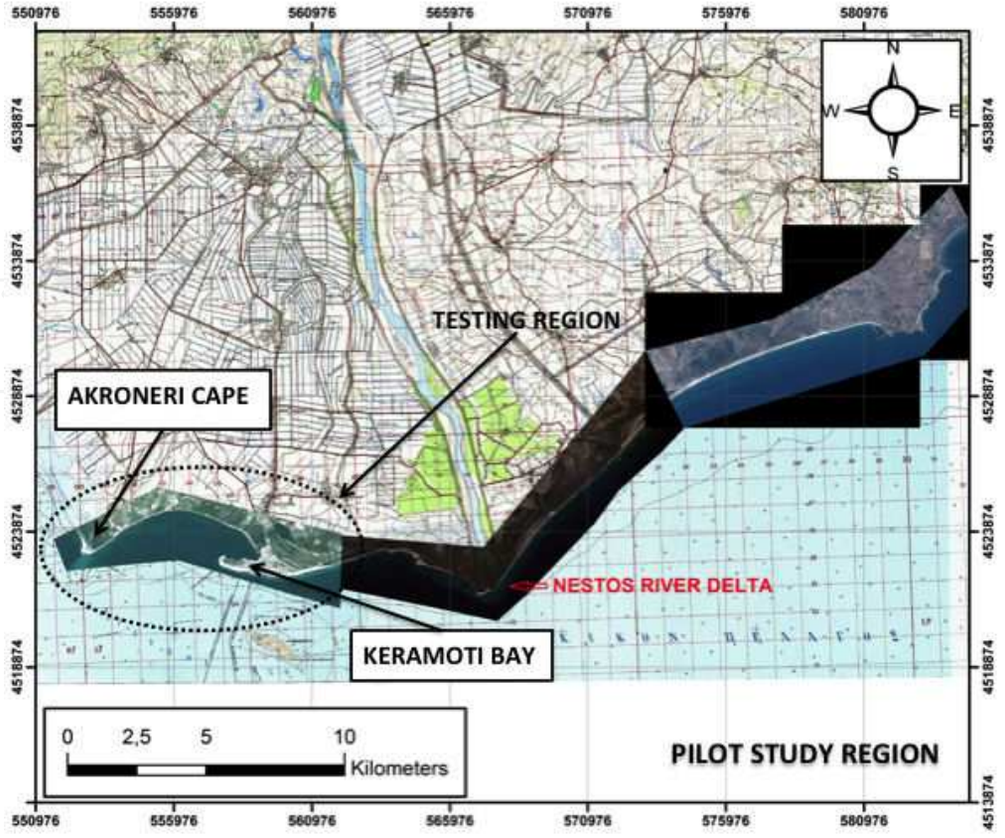

Figure 2. Pilot study region for shoreline change monitoring and selected region for testing the accuracy and effectiveness of the adopted shoreline change monitoring methodology

2.3.3. Ortho-rectification of aerial photographs and extraction of digital shoreline

The ortho-rectification of the available old aerial photographs of the region and the digital extraction of the corresponding shoreline was conducted with the ArcMap software of the ArcGIS 9 package. The basic stages of the proposed procedure are summarized below:

- The aerial photographs were scanned and digitally imported into the ArcMap database in order to be ortho-rectified in the EGSA 87 coordinate system, using as GCPs points that were both visible in the aerial photographs as well as in the ortho-rectified map background. A total number of 6-8 GCPs were used for each aerial photograph.
- A surface analysis was then performed in the aerial photographs and automatic contours were generated.
- The contour that corresponded to the dividing line between land and sea pixels was manually selected by visual inspection and digitally extracted as the shoreline position in the year 1945.

Figure 3 (a) illustrates the digitally extracted shoreline for the testing region (year 1945) superimposed on the corresponding aerial photograph where the adequate accuracy and the validity of the extraction method described above can be clearly seen.

http://dx.doi.org/10.5772/61459

2.3.4. Step 3 – Ortho-rectification of high-resolution satellite images and extraction of digital shoreline

The digital shoreline extraction from the ortho-rectified, high-resolution, satellite images of the region was also conducted using the ArcMap software of the ArcGIS 9 package. The basic stages are summarized below:

- Ortho-rectified, QB satellite images of the pilot study region were selected and ordered from the archive database of GEOMED LTD, one of the authorized resellers of these images, in Greece.
- The proposed 4-band satellite images were then imported into the ArcMap database in the EGSA 87 coordinate system and adjusted to the infrared channel.
- The well-known "Natural Breaks (Jenks)" pixel classification method was then applied on the images, from the "spatial analyst" tool of the ArcMap software, in order to separate sea and land pixels.
- Then a contour line was automatically inserted at the interface of the classified sea and land pixels and digitally extracted as the shoreline.
- Figure 3 (b) illustrates the digitally extracted shoreline for the testing region (year 2002) superimposed on the corresponding satellite image, where the adequate accuracy and the validity of the extraction method described above can be clearly seen.

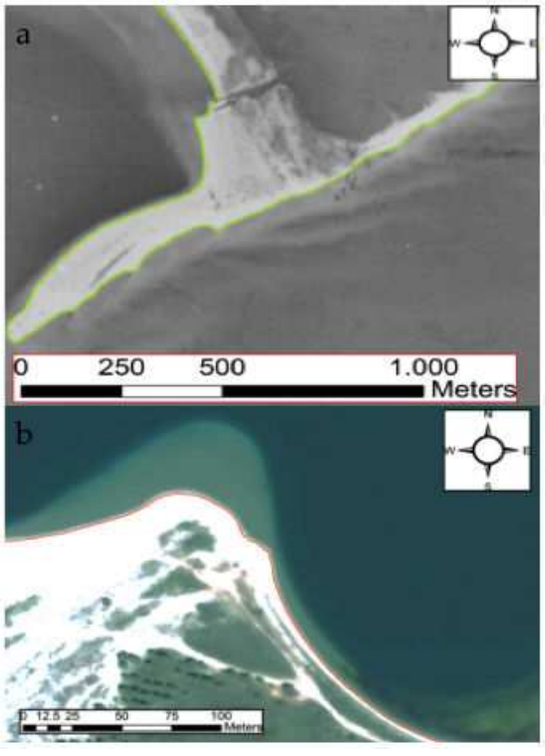

Figure 3. (a) Digitally extracted shoreline from the aerial photograph that corresponds to the test region (year 1945), superimposed on the aerial photograph. (b) Digitally extracted shoreline from the high-resolution satellite images that correspond to the test region (year 2002), superimposed on the satellite image

2.3.5. Step 4 – DGPS field measurements and extraction of digital shoreline

The DGPS field measurements were conducted using a high-resolution DGPS system that consists of two GPS receivers. A static receiver that was installed at various, known, benchmark trigonometric points of the region that were preinstalled by the HMGS and a rover (mobile) receiver which was used for the surveying of the shoreline in the field. The recorded data points from the rover receiver along the shoreline were then postprocessed and extracted in AutoCAD files in the EGSA 87 coordinate system and finally imported superimposed at the ArcMap database. The accuracy of the DGPS measurements according to the specifications of the proposed equipment was of the order of few centimetres. However, this was double-checked and verified using GCPs with known coordinates.

2.4. Quantitative and qualitative results from the application of the selected shoreline change monitoring methodology at the entire pilot study area

2.4.1. General

In the present subsection, quantitative and qualitative results from the application of the proposed methodology to the entire pilot study region are presented and discussed in detail. Figure 4 illustrates indicatively some stages of the application for the entire pilot study area.

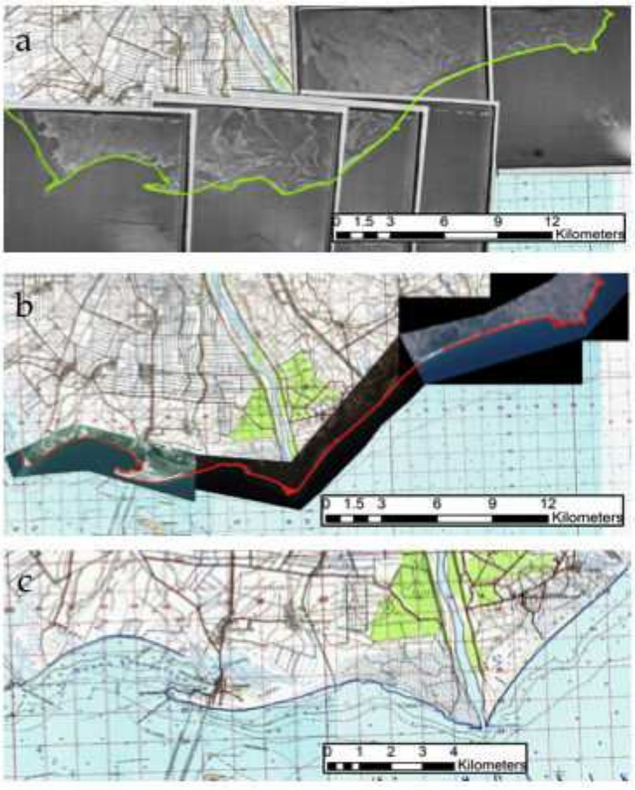

Figure 4. (a) Digitally extracted shoreline from aerial photographs (year 1945) for the entire pilot study region, superimposed on the aerial photographs. (b) Digitally extracted shoreline from satellite images (year 2002) for the entire pilot study region, superimposed on the satellite images. (c) Digitally extracted shoreline from DGPS measurements (year 2007) for the entire pilot study region, superimposed on the common working background

http://dx.doi.org/10.5772/61459

2.4.2. Calculation of erosion/accretion balance for the region of the Nestos River delta and the adjacent shorelines, before and after the construction of the dams

In order to investigate the erosion/accretion balance between the years 1945 and 2002 (time period before the construction of the dams) and the years 2002 to 2007 (time period after the construction of the dams), polygons that represent eroded and accreted areas were extracted from the ArcMap database. These are illustrated in Figure 5 for the two different time periods, respectively. The boundaries of these polygons are defined by the nonintersecting parts of the two digitally extracted shorelines in each of the examined time periods.

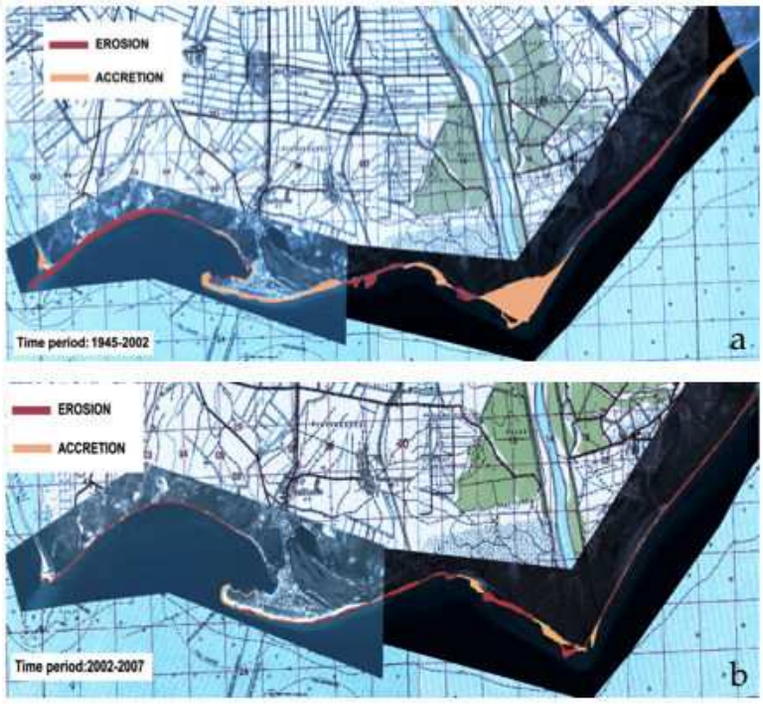

Figure 5. Eroded/accreted areas for the time periods 1945-2002 and 2002-2007

The resulting erosion/accretion balance expressed in m^2 as well as in percentages relative to the total area, is summarized in Table 3.

1945-2002	
Erosion area (m^2)	Accretion area (m^2)
1335027.90	2242207.82
Erosion percentage (%)	Accretion percentage (%)
37.32	62.68
2002-2007	
Erosion area (m^2)	Accretion area (m^2)
374892.96	243453.14
Erosion percentage (%)	Accretion percentage (%)
60.63	39.37

Table 3. Areas of erosion and accretion in the pilot study region, for the time periods 1945-2002 and 2002-2007

As it can be observed, from the year 1945 up to the year 2002 and for the considered shoreline (total length of 25 km), the erosion was about 1335028 m^2 (23421 m^2 per year) and the accretion 2242208 m^2 (39337 m^2 per year), i.e., the overall balance of the eroded/accreted areas from 1945 to 2002, indicates that accretion is the dominant mechanism covering a total area almost 1.7 times bigger than the corresponding area of the eroded parts. In other words, accretion dominates erosion by 25.36%. On the other hand, examining the same shoreline region from 2002 to 2007, the erosion was about 374893 m^2 (74979 m^2 per year) and the accretion 243453 m^2 (48691 m^2 per year), i.e., the erosion mechanism dominates accretion by approximately 21.26%. Therefore, it can be concluded that the dramatic decrease in the sediments supplied directly to the Nestos River basin outlet and indirectly to the neighboring coast, due to the construction and operation of the considered reservoirs, has almost inversed the previous state regarding the erosion/accretion balance in the considered region, just within 5 years of the construction of the dams. This finding evaluates the direct effect of the construction of the Thisavros and Platanovrysi Dams, to the erosion increase in the coastal region of the Nestos River delta and the adjacent shorelines.

2.5. New shoreline

As mentioned previously, for the purposes of the present investigation it was deemed appropriate to also extract a more recent shoreline (year 2013), in order to perform a comparison with the shorelines of the years 2002 and 2007, aiming at the quantitative investigation of the dynamic evolution of the examined coastal region, from the shoreline erosion point of view [14].

For this purpose, additional DGPS field measurements were conducted, following the same methodology and time period (spring) with the corresponding field measurements that were conducted in the year 2007. This more recent shoreline (2013) consists of three subregions: the Akroneri Cape region, the Keramoti Bay region and the region in the vicinity of the Nestos River delta.

The erosion/accretion balance between the shorelines of 2002-2007, 2007-2013, and 2002-2013 is illustrated in detail for these three subregions (Akroneri Cape in Figure 6, Keramoti Bay in Figure 7, and Nestos River delta in Figure 8).

As it can be macroscopically observed from Figure 6, in Akroneri Cape region, the eroded areas (red color) dominate the accreted areas (green color) in each one of the examined time periods. Examining both the subsequent periods 2002-2007 and 2007-2013 as well as in total the period from 2002 (considered period for reservoir construction and operation) to 2013 (most recent situation), in comparison with the initially examined period (2002-2007), it is characteristic that as years are passing, areas that in the first period were under relatively severe accretion are suffering in the subsequent periods from quite noticeable erosion.

Almost the same trend is also observed in the region of Keramoti Bay, as it can be concluded by comparing the same time periods as previously (Figure 7). In more detail, while in the initial

http://dx.doi.org/10.5772/61459

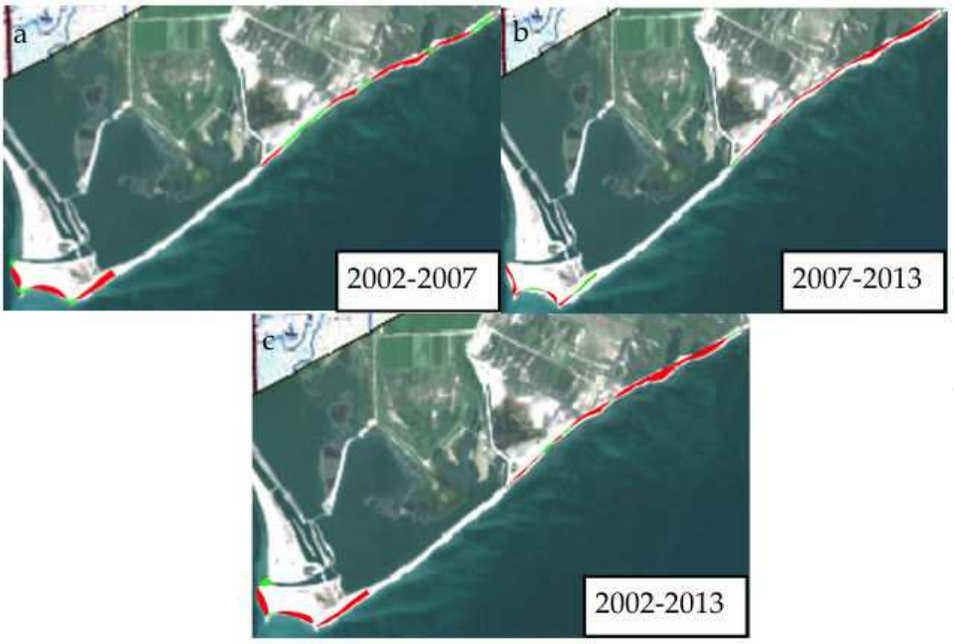

Figure 6. Erosion (red color) /Accretion (green color) balance at Akroneri Cape region

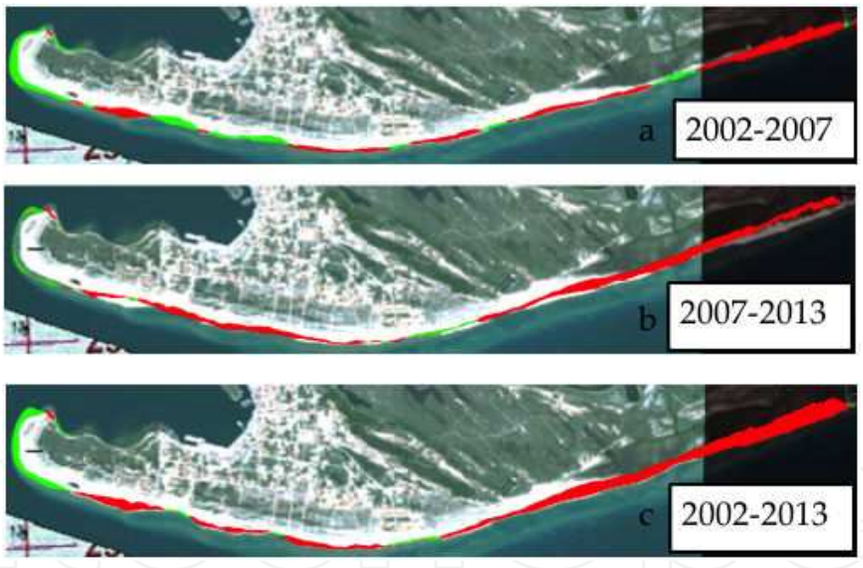

Figure 7. Erosion (red color) /accretion (green color) balance at Keramoti Bay region

time period quite big areas of erosion as well as accretion can be traced, in the subsequent time period the areas that were initially under severe accretion, are now subjected to light accretion or even under considerable erosion. Accordingly, the areas that were initially subjected to considerable erosion, present now a more intense shoreline retreat.

Regarding the region in the vicinity of the Nestos River delta, despite the fact that the shoreline presents a more intense and dynamic evolution, also in this case the initially presented

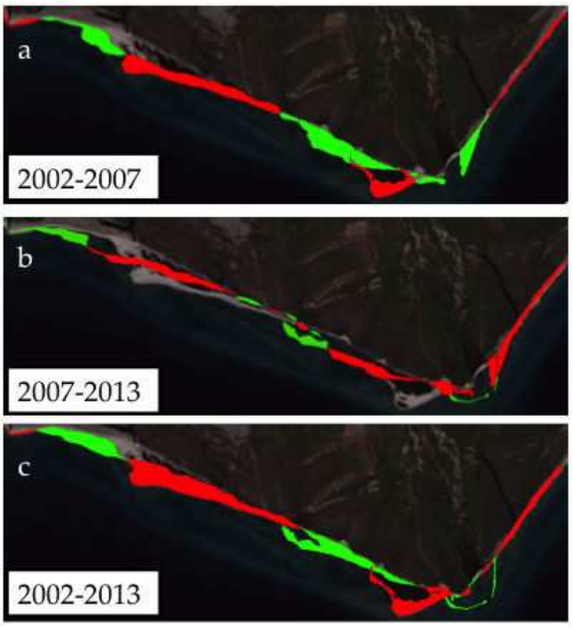

Figure 8. Erosion/accretion balance in the region of the Nestos River delta

(2002-2007) erosion/accretion balance in the subsequent time period (2007-2013) has been disturbed, indicating an increasing trend in the areas that are subjected to erosion with respect to the areas that are subjected to accretion.

All the above macroscopic observations are quantitatively summarized in Figure 9, where the percentages of erosion and accretion for the two subsequent time periods as well as for the entire examination period are depicted for each one of the examined regions.

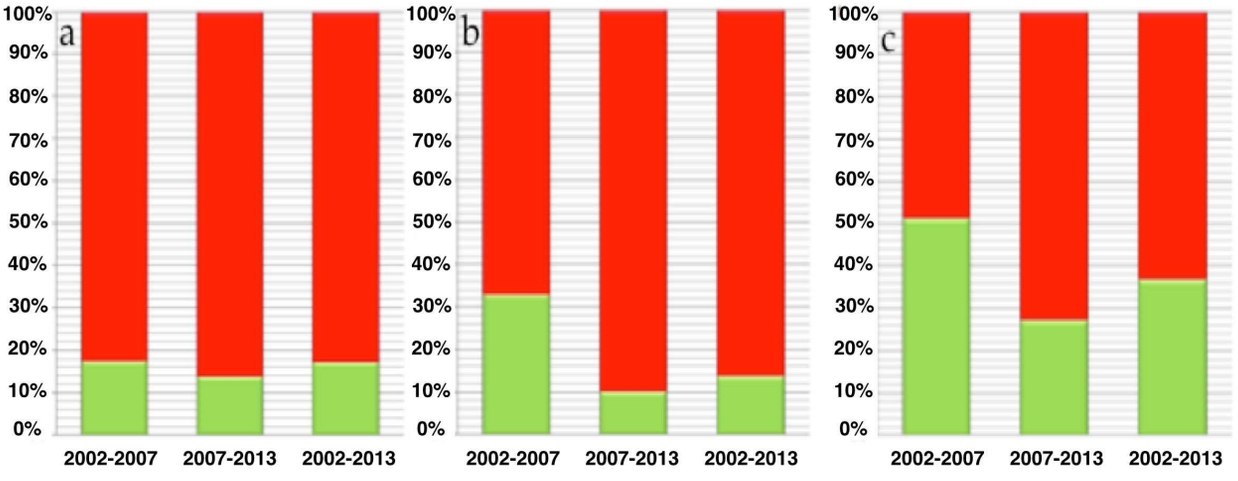

Figure 9. Erosion (red color) /accretion (green color) percentages for the considered time periods, at Akroneri Cape region (a), at Keramoti Bay region (b) and the Nestos River delta region (c)

http://dx.doi.org/10.5772/61459

As it can be observed in all three considered regions, the erosion percentage in the time period 2007-2013 shows a significant increase in comparison with the previous time period (2002-2007). At Akroneri Cape region, an increase in the areas subjected to erosion by just 4% is observed. On the other hand, in the regions of Keramoti Bay and Nestos River delta, the corresponding increase reaches 23% and 24%, respectively, within just 6 years. It is also characteristic that in the case of the Nestos River delta, while in the time period 2002-2007 an erosion/accretion balance is observed, in the subsequent time period erosion predominates accretion by a considerable percentage. All the above quantitative observations can lead to the conclusion that the predomination of erosion with respect to accretion, after the construction and operation of the two reservoirs (year 2002), shows a continuously increasing trend.

3. Evaluation of sediment management techniques for coastal erosion reduction

3.1. Overview

In this third part of the present chapter, the effect of sediment removal by dredging and flushing from the Platanovrysi Reservoir downstream is investigated, in order to evaluate the increase in the sediment budget that reaches the outlet basin, as this increase can contribute to the reduction of shoreline erosion. For this purpose, the previously validated and applied mathematical model (RUNERSET - RUNoff ERosion SEdiment Transport) is modified accordingly in order to take into account sediment dredging and flushing applications. The proposed modifications involve the addition of different amounts of eroded material (sediment) in the subbasin that lies directly downstream of the Platanovrysi Reservoir for dredging processes as well as the inclusion of a flushing discharge. In more detail, a parametric investigation is conducted using a wide series of simulated scenarios, aiming to identify the optimum periods that dredging and flushing can be applied in order to maximize the increase of the sediment that is transported and reach the basin outlet [13].

3.2. Application of sediment dredging technique to Platanovrysi Reservoir

In order to investigate the possible contribution of the mechanical removal (dredging) of sediment from the Platanovrysi Reservoir, and its deposition in the subbasin downstream of the Platanovrysi Dam, the mathematical model RUNERSET [10] was accordingly modified. In more detail, the proposed modification involves the addition of different, eroded sediment amounts in Subbasin 7 (Figure 1) for specific months of each year, for the time period 1980-1990.

A total number of 888 simulations were conducted for the years 1980-1990 assuming the following scenarios: application of dredging in each month of each year and for various amounts of sediment removal. Initially, diagrams of the total annual amount of sediment that reaches the basin outlet, versus the amount of sediment that was removed by dredging from the Platanovrysi Reservoir, were constructed. Figure 10 illustrates indicatively these diagrams for two of the considered years.

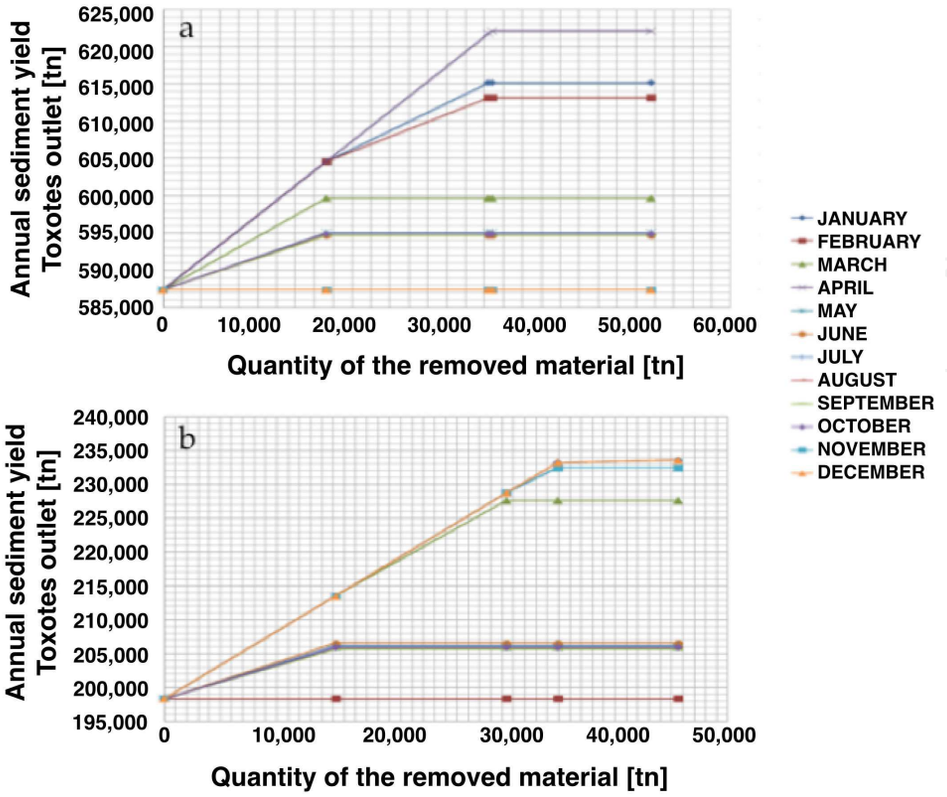

Figure 10. Indicative results from simulated dredging scenarios for the years 1981 (a) and 1986 (b)

From these diagrams it is obvious that for dredging scenarios in specific months of the year, the total annual sediment amount that reaches the basin outlet is higher than the corresponding amount in the rest of the months. Therefore, the months of the year can be clearly classified as "effective" and "ineffective" for a dredging application. In more detail, from the overall analysis of the simulation results, it can be concluded that January, February, March, April, November, and December can be, in general, characterized as "effective" months, while for the time period from May to October (ineffective months), a potential dredging application would not alter significantly the annual sediment amount that reaches the outlet of the river. The month classification in "effective" and "ineffective" is summarized schematically in Figure 11 (a), where the additional annual amount of dredged sediment that reaches Toxotes outlet of the river (Figure 1), is plotted against the amount of sediment that was removed in the specific month of the year in each case, for the overall simulated scenarios.

It has also to be mentioned that for amounts of sediment removal up to 35000 tn and for dredging scenarios in the effective months of the year, the ratio of the additional sediment amount that reaches Toxotes outlet, to the removed sediment amount, is equal to unity. This indicates that, generally, up to a limiting value of 35000 tn of dredged sediment from the Platanovrysi Reservoir, in an effective month, all of this removed amount of sediment will reach Toxotes outlet. Moreover, from a certain amount of removed sediment and above, there is not any change in the amount of sediment that reaches the basin outlet. This indicates that there is a maximum transport quantity of dredged material that the Nestos River can transport

http://dx.doi.org/10.5772/61459

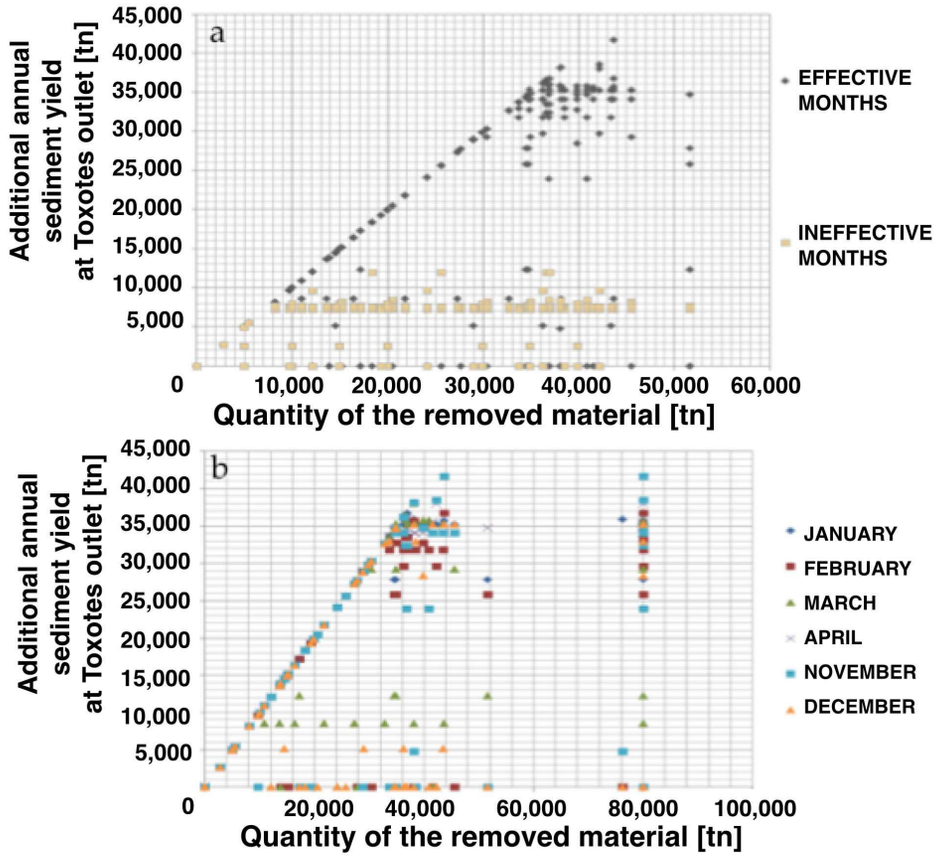

Figure 11. (a) Effective and ineffective months for dredging application, (b) Result of dredging application during the effective months of the year (the data points represent the overall simulated scenarios)

up to the basin outlet. This limiting amount varies accordingly for each month. Therefore, it is vital to define the month of the year in which this sediment transport quantity is maximized. Figure 11 (b) indicates that the maximum value of sediment surplus that reaches the basin outlet, takes place if dredging is applied in November.

However, for November there are also a lot of simulations that resulted in a zero sediment surplus at the basin outlet (in some of the overall simulated years). This means that while the Nestos River can transport the maximum amount of sediment that reaches the basin outlet, if the dredging application is performed during November for a certain year, it is also possible in a different year that no sediment at all reaches the outlet. Therefore, an additional classification of the "effective" months to "consistent" and "inconsistent" must be conducted. According to the diagram of Figure 11 (b), the months January and April can be characterized as "consistent," while February, March, November, and December can be characterized as "inconsistent."

In order now to investigate the most "effective" and "consistent" month of the year for applying sediment dredging, between January and April, a direct comparison of these two months was conducted. For this purpose, the overall results from all the simulated years (1980-1990) and for all the amounts of dredged sediment were collected, for January and April.

The quantitative analysis of the proposed simulation results indicated that the overall sediment dredging performance of these two months could be classified into three distinct parts. The first part refers to dredging scenarios with sediment removal up to 34400 tn, in which the performance of each month with respect to the amount of sediment surplus that reaches the basin outlet is the same, having a value of 100%. The second and third parts consist of dredging scenarios with sediment removal from 34400 tn up to 36150 tn and greater than 36150 tn, respectively. In these last two parts of the collected data, the performance of each month is different, having values also lower than 100%. Taking into account the fact that the Nestos River cannot in general transport to the basin outlet dredged sediment amounts greater than 35000 tn, the third part of the resulting data was neglected from the comparison process. For the proposed comparison, the mean value of the dredged sediment amount that did not reach the basin outlet was taken as the effectiveness criterion, while the corresponding standard deviation was used as the criterion for consistency. The overall analysis from the comparison between January and April is summarized in Table 4. It is obvious that April can be assumed as the most suitable month of the year for a dredging application to the Platanovrysi Reservoir. It is also worth mentioning that the sediment amount of 35000 tn, that is, the maximum amount of dredged sediment that can reach the outlet of the Nestos River, is equal to 2.46% of the mean annual sediment yield of the river at its outlet, before the construction of the considered dams, and the 10.95% of the mean annual yield of the river after the construction and operation of the reservoirs. Finally, this sediment amount also constitutes the 11.53% of the mean annual sediment yield that reaches the Platanovrysi Reservoir.

	Quantity of removed material [tn]	**Additional annual sediment yield at Toxotes outlet [tn]**			
		JANUARY	**Nondelivered sediment quantity [tn]**	**APRIL**	**Nondelivered sediment quantity [tn]**
34400	27806	6594	34400	0	
34625	34626	-1	34625	0	
34744	27806	6938	34744	0	
34825	34825	0	34102	723	
34903	34902	1	34101	802	
36150	35238	912	36150	0	
Mean value	34941.17	32533.83		34687	
Mean attribution [%]	–	93.11		99.27	
		Mean value	2407.33	Mean value	254.17
		Standard deviation	3396.38	Standard deviation	394.55

Table 4. Comparison of effectiveness and consistency between January and March for dredging application

http://dx.doi.org/10.5772/61459

3.3. Application of sediment flushing to Platanovrysi Reservoir

In order to investigate the possibility of minimizing shoreline erosion due to the construction of the proposed dams, with the application of flushing, the mathematical model RUNERSET was accordingly modified, in order to take into account the corresponding flushing discharge. Also in these series of simulations, the model was applied for the years 1980–1990. For the calculation of the flushing discharge, Equation (12) was used assuming that the sediment flushing discharge is known [11]:

$$Q_f = \left(\frac{Q_s}{3,5 \cdot 10^{-3} \cdot \left(S \cdot 10^4 \right)^{1,8}} \right)^{1/1,2} \quad Q_f = \left(\frac{Q_s}{3,5 \cdot 10^{-3} \cdot \left(S \cdot 10^4 \right)^{1,8}} \right)^{1/1,2} \quad Q_f = \left(\frac{Q_s}{3,5 \cdot 10^{-3} \cdot \left(S \cdot 10^4 \right)^{1,8}} \right)^{1/1,2} \tag{12}$$

where Qs is the removed sediment discharge from the reservoir during a flushing event (tn/s); S is the bottom slope along the flushing channel, assuming that the flow is uniform and therefore the slope of the energy line and the flow line coincide; and Q_f: is the flushing discharge (m^3/s).

In order to determine the optimum month of the year for the application of flushing in the Platanovrysi Reservoir, a series of simulations were performed with a sediment flushing discharge of 0.0135 tn/s (that corresponds to the value of 35000 tn) and for flushing events occurring in different months. The results are summarized in Table 5.

PERCENTAGE OF FLUSHED SEDIMENT THAT REACHES TOXOTES OUTLET [%]											
1980	**1981**	**1982**	**1983**	**1984**	**1985**	**1986**	**1987**	**1988**	**1989**	**1990**	
JAN	**99.99**	**79.50**	**100.00**	**100.00**	**100.00**	**99.99**	**99.88**	**99.99**	**99.91**	**100.00**	**100.00**
FEB	95.71	73.78	90.94	93.72	0.00	99.99	0.00	0.00	84.48	90.86	90.97
MAR	99.99	35,20	100.00	100.00	0.00	24.55	83.59	99.99	0.00	100.00	100.00
APR	**99.99**	**99,22**	**99.22**	**97.44**	**100.00**	**97.42**	**97.59**	**0.00**	**99.91**	**97.43**	**97.45**
MAY	34.26	21.77	24.06	22,88	21.46	21.98	21.58	22.54	27.61	21.70	21.55
JUN	20.83	20.91	20.92	0.00	20.89	20.83	23.58	23.68	0.00	20.84	20.86
JUL	21.40	21.48	21,78	7.45	21.46	21.69	22.43	21.68	21.61	21.70	21.55
AUG	21.40	21.48	21.49	21.56	21.46	21.69	21.58	21.68	21.61	21.70	21.55
SEP	20.83	20.91	20.92	20.85	20.89	20.83	20.72	20.82	20.75	20.84	20.86
OCT	21.40	21.48	21.49	21.56	21.46	21.69	21.58	21.68	20.75	0.00	21.55
NOV	92.56	0.00	68.36	99.15	97.48	99.99	97.59	13.68	99.91	0.00	97.45
DEC	0.00	0.00	0.00	81.18	100.00	99,99	99.88	0.00	0.00	94.00	14.58

Table 5. Results from simulations of flushing scenarios for different months of the year

It is obvious that the optimum month for the application of a flushing event, in order to maximize the overall flushed sediment amount that reaches the basin outlet, and therefore decreases the indirect shoreline erosion, is January and not April (as in the corresponding investigation for the application of dredging). However, April is found to be the second most effective month. In the literature it is stated that in order to maximize the amount of sediment that is removed from a reservoir and therefore restore its storing capacity, a flushing event will be more effective if it occurs at the beginning of the ice melting period [11]. Therefore, from this point of view, April could be characterized as the optimum month of the year for the application of a flushing event.

In order to calculate the river's maximum transport quantity of flushed sediment at the outlet of its basin, additional scenarios of continuous through each year flushing events were simulated. For this purpose, the mathematical model RUNERSET was further modified in order to take into account sediment flushing discharge equal to 0.1 tn/s, a value much greater than the previously identified critical value of 0.0135 tn/s. From the analysis of the results it is found that the Nestos River could transport to the basin outlet approximately 200000 tn of additional sediment, if the flushing of sediment was applied continuously during the whole year. It is worth mentioning that this amount constitutes the 62% of the mean annual sediment yield today.

Taking into account that the application of flushing could be more effective, at least from the point of view of limiting shoreline erosion, during certain months of the year (time period from November to April), additional continuous flushing scenarios were simulated for the period of the six more effective months of the year for each of the considered years (1980-1990). The overall results are summarized in Figure 12.

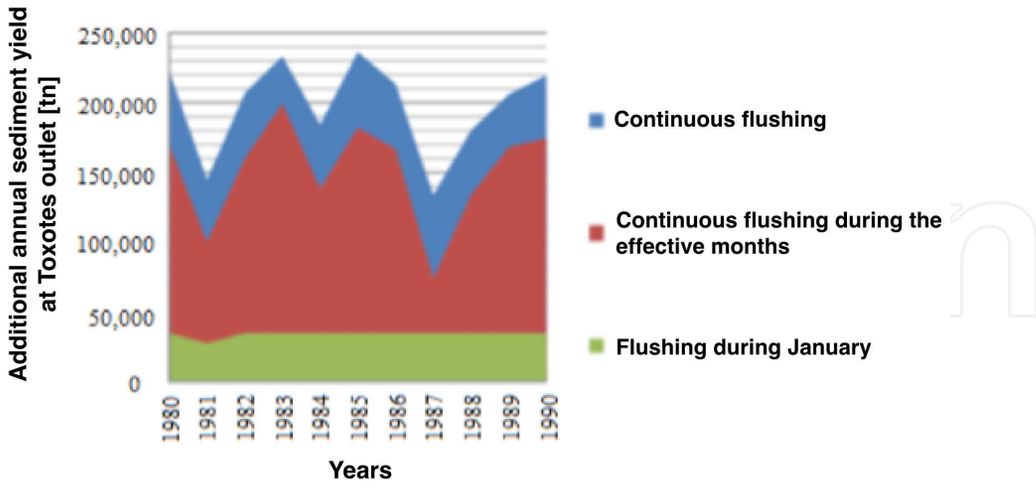

Figure 12. Results from simulated flushing scenarios

Examining Figure 12, it can be concluded that in the case that the continuous flushing event happens during the six of the most effective months of the year, the amount of sediment that reaches the basin outlet of the Nestos River reaches the 76.5% of the corresponding amount in

http://dx.doi.org/10.5772/61459

the case of continuous flushing throughout the whole year. Moreover, in the case that the sediment flushing event is applied only during January the amount of sediment that reaches the outlet constitutes the 17.35% of the maximum possible amount (continuous flushing throughout the year). This amount is also equal to the 73.5% of the amount that would reach Toxotes outlet, in the case of a continuous flushing event during the noneffective months of the year (period from May to October).

3.4. Comparison of the considered sediment removal methods

In order to select the optimum of the two examined methods, a comparison was conducted by collecting the maximum amount of sediment that reaches the basin outlet of the Nestos River, that are attributed, if each method is applied in its optimum identified month of the year; April for the application of mechanical sediment removal, and January for the application of sediment flushing.

In order to calculate these quantities, a sediment discharge (dredging/flushing) greater than the previously used values of 35000 tn for the case of dredging and 0.0135 tn/s for the case of flushing was assumed. In more detail, the mathematical model was further modified in order to take into account a sediment discharge of Q_s=289200 tn and q_{sf}=0,1 tn/s, since it was proven that for values generally above 35000 tn (approximately 0.0135 tn/s for the case of a flushing event with a duration of 30 days), the results of the simulations did not change. The results of the proposed comparison are summarized diagrammatically in Figure 13.

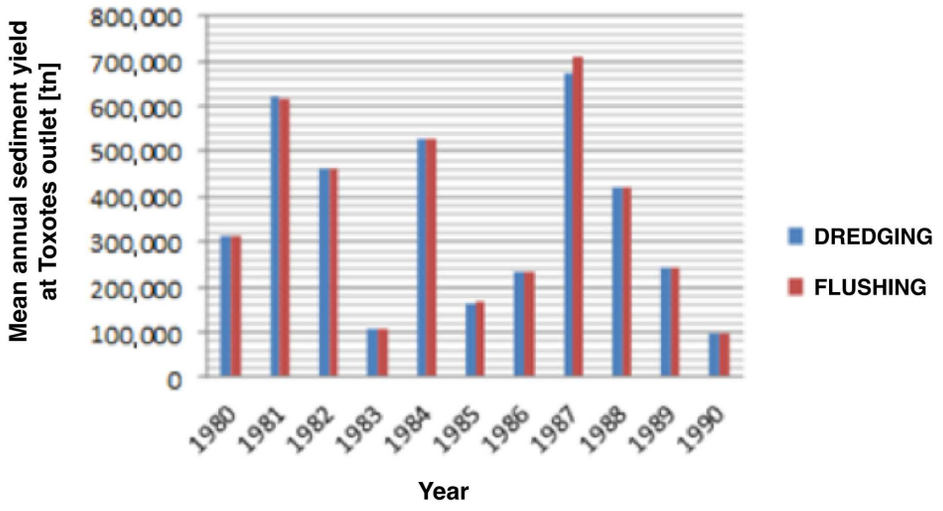

Figure 13. Comparison between dredging and flushing

It can be seen that flushing seems to perform slightly better than dredging but in a degree that cannot be chosen as the optimum method. Therefore, in order to choose the optimal method for the aim of the present investigation, other criteria such as technical difficulties in their application as well as cost of application should be taken into consideration.

4. Conclusions

Coastal erosion that is generated by the reduction of the annual sediment yield at river outlets due to the construction of dams constitutes one of the main environmental problems in many parts of the world. Nestos is one of the most important transboundary rivers, characterized by its great biodiversity. The Nestos River flows through two European countries, Bulgaria and Greece, and discharges its water into the Aegean Sea. In the Greek part of the river, two dams, the Thisavros Dam and the Platanovrysi Dam, have already been constructed and started operating in 1997 and 1999, respectively. The construction of the dams implies a reduction of sediment yield at the outlet of the Nestos River basin and the alteration of the sediment balance of the basin in general, which results in coastal erosion.

The present chapter deals with the assessment of reservoir sedimentation effect on the coastal erosion for the case of the Nestos River delta and the adjacent shorelines, through mathematical modeling, remote sensing techniques, and field surveying. The mathematical model is applied for the estimation of the sediment yield reduction at the outlet of the river due to the subsequent sediment accumulation within the reservoirs, while a shoreline change monitoring methodology is applied for the estimation of the alteration of the erosion/accretion balance in the wider coastal region of the Nestos River delta, examining the proposed balance in two different time periods, before and after the construction of the dams.

The mathematical model results indicate that the construction of the considered dams has caused a dramatic decrease (about 83%) in the sediments supplied directly to the basin outlet (delta) and indirectly to the neighboring coast. Comparing the overall balance of the eroded and accreted areas in the region, before and after the construction and operation of the reservoirs, it can be concluded that the decrease in the sediments supplied directly to the Nestos River basin outlet and indirectly to the neighboring coast, has almost inversed the previous situation (where accretion predomin;ated erosion by 25.36%), just within 5 years of the construction of the reservoirs, with erosion now predominating accretion by 21.26%. The extraction of a more recent shoreline and the corresponding comparison with the previously identified shoreline states clearly indicates a continuously increasing trend in the predomination of erosion in relation to accretion.

Based on the above, it emerges that the construction and operation of the Thisavros and Platanovrysi Reservoirs have significantly increased coastal erosion in the Nestos River delta and the adjacent shorelines. This fact, together with the anticipated rise of sea level, may pose a great problem to the coastal area resources, threatening the local communities and ecosystems of the considered region. Therefore, it is necessary to further investigate the sediment budget within the estuarine and the adjacent coastal systems and to further monitor erosion/accretion trends of the region for the coming decades.

In the present chapter also, a previously validated and applied mathematical model is modified accordingly in order to take into account the application of sediment dredging and flushing in a reservoir of river hydrological basin. The modified model is applied for the case of the Nestos River (Greece) in order to identify the optimum sediment removal scenario in a

certain reservoir (Platanovrysi Reservoir) upstream of the considered river outlet (Toxotes outlet), in order to maximize the amount of sediment that reaches the delta of the river. In more detail, a wide series of parametric simulation scenarios is performed, aiming to identify the optimum periods that the dredging and flushing can be applied. From the overall analysis of the simulation results, a definite classification of the months into "effective" and "ineffective" as well as into "consistent" and "inconsistent" with respect to the total amount of removed sediment that reaches the basin outlet is made. It is also found that the considered river has a maximum transport capacity of the removed material, regardless of the further increase of the dredged and/or flushed sediment capacity from the identified limiting value. A comparison between the two considered methods identified flushing to be slightly more effective than dredging.

Finally, the overall results of the present investigation indicate that the proposed modified mathematical model can serve as a quite effective and useful tool that can be applied for similar investigations at various river basins worldwide and it could also be incorporated into the early design stages of new reservoirs that are going to be constructed, estimating the amount of sediment discharge that needs to pass through the reservoir in the downstream part of the river basin in order to minimize the unavoidable deltaic and adjacent shoreline erosion.

Acknowledgements

The authors would like to acknowledge the financial support from the Research Project, INTEREG IIIC BEACHMED-e, "Strategic management of beach protection for sustainable development of Mediterranean coastal zones."

Author details

Manolia Andredaki[1], Anastasios Georgoulas[2*], Vlassios Hrissanthou[1] and Nikolaos Kotsovinos[1]

*Address all correspondence to: anastasios.georgoulas@gmail.com

1 Department of Civil Engineering, Democritus University of Thrace, Xanthi, Greece

2 Department of Engineering, University of Bergamo, Dalmine (BG), Italy

References

[1] Ly C.K. 1980, The role of the Akosombo Reservoir on the Volta river in causing coastal erosion in central and eastern Ghana (West Africa), *Mar Geol*, Vol. 37, pp. 323-332.

[2] Chen X. and Zong Y. 1998, Coastal erosion along the Changjiang deltaic shoreline, China: history and prospective, *Estuar Coast Self Sci*, Vol. 46, pp. 733-742.

[3] El-Raey M., Sharaf El-Din S.H, Khafagy A.A. and Abo Zed A.I. 1999, Remote sensing of beach erosion/accretion patterns along Reservoirietta-Port Said shoreline, Egypt, *Int J Remote Sensing*, Vol. 20, No. 6, pp. 1087-1106.

[4] Malini B.M. and Rao K.N. 2004, Coastal erosion and habitat loss along the Godavari delta front – a fallout of reservoir construction (?), *Curr Sci*, Vol. 87, No. 9, pp. 1232-1236.

[5] Chen X., Yan Y., Fu R., Dou X. and Zhang E. 2008, Sediment transport from the Yangtze River, China, into the sea over the Post-Three Gorge Reservoir Period: A discussion, *Quater Int*, Vol. 186, pp. 55-64.

[6] Liu C., Sui J. and Wang Z. 2008, Sediment load reduction in Chinese rivers, *Int J Sed Res*, Vol. 23, pp. 44-55.

[7] Huang G. 2011, Time lag between reduction of sediment supply and coastal erosion, *Int J Sed Res*, Vol. 26, pp. 27-35.

[8] Zhang W., Mu S., Zhang Y. and Chen K. 2011, Temporal variation of suspended sediment load in the Pearl River due to human activities, *Int J Sed Res*, Vol. 26, pp. 487-497.

[9] Samaras A.G. and Koutitas C.G. 2008, Modelling the impact on coastal morphology of the water management in transboundary river basins: The case of River Nestos, *Manag Environ Qual: Int J*, Vol. 10, No. 4, pp. 455-466.

[10] Andredaki M., Georgoulas A., Hrissanthou V. and Kotsovinos N. 2014, Assessment of reservoir sedimentation effect on coastal erosion in the case of Nestos River, Greece, *Int J Sed Res*, Vol. 29, pp. 34-48.

[11] Morris G.L. and Fan J. 1998, *Reservoir Sedimentation Handbook*. New York: McGraw-Hill Book Co.

[12] Basson G. and Rooseboom A. 1997, Dealing with reservoir sedimentation. South African Water Research Commission.

[13] Andredaki M., Georgoulas A. and Hrissanthou V. 2014, Sediment management in reservoirs in order to reduce shoreline erosion: The case of Nestos River, Greece, 4th International Symposium on Sediment Management, 14-16 September, Ferrara, Italy (Paper ref. no. 112).

[14] Andredaki M. 2014, Effect of reservoir sedimentation on shoreline erosion – The example of Nestos River, PhD Thesis, Sector of Hydraulic Structures, Department of Civil Engineering, Democritus University of Thrace, Xanthi, Greece.

[15] Giakoumakis S., Tsakiris G. and Efremides D. 1991, On the rainfall-runoff modeling in a Mediterranean island environment. In: *Advances in Water Resources Technology*, ed. by G. Tsakiris, Balkema, Rotterdam, pp. 137-148.

[16] SCS (Soil Conservation Service) 1972, *National Engineering Handbook*. Section of Hydrology, SCS, Washington DC, USA.

[17] Doorenbos J. and Pruitt W. O. 1977, Crop water requirements. FAO, Irrigation and Drainage Paper 24 (revised). FAO, Rome, Italy.

[18] Thornthwaite C. W. 1948, An approach towards a rational classification of climate. *Geographic Rev*, Vol. 38, pp. 55-94.

[19] Schmidt J. 1992, Predicting the sediment yield from agricultural land using a new soil erosion model. Proceedings 5th International Symposium on River Sedimentation, ed. by P. Larsen and N. Eisenhauer, Karlsruhe, Germany, pp. 1045-1051.

[20] Yang C. T. 1973, Incipient motion and sediment transport. *J Hydraul Div*, ASCE, Vol. 99, No. 10, pp. 1679-1704.

[21] Gergov G. 1996, Suspended sediment load of Bulgarian rivers. *GeoJournal*, Vol. 40, No. 4, pp. 387-396.

[22] Kapona E. and Tona E. 2003, Computation of the inflowing sediments into Thisavros Reservoir of Nestos River. Diploma Thesis, Department of Civil Engineering, Democritus University of Thrace, Xanthi, Greece (in Greek).

[23] Klisiari A. 2002, Computation of the inflowing sediments into Platanovrysi Reservoir of Nestos River. Diploma Thesis, Department of Civil Engineering, Democritus University of Thrace, Xanthi, Greece (in Greek).

[24] Hrissanthou V. 2002, Comparative application of two erosion models to a basin. *Hydrol Sci J*, Vol. 47, No. 2, pp. 279-292.

IntechOpen